Shock wave interaction with convex circular cylindrical surfaces

BERIC W. SKEWS[1]† AND HARALD KLEINE[2]

[1]School of Mechanical, Industrial, and Aeronautical Engineering, University of the Witwatersrand, Johannesburg 2050, South Africa

[2]School of Engineering and Information Technology, University of New South Wales, Australian Defence Force Academy, Canberra, ACT 2600, Australia

The reflection of shock waves off cylindrical surfaces of different radii is examined with the help of time-resolved flow visualization. The primary diagnostic is a newly developed technique based on the tracking of deliberately introduced small perturbations in the flow. The main focus of the investigation is to determine at which position the shock wave receives information about the shape of the wall that it reflects off. In the pseudo-steady shock reflection off a plane wall, it is commonly accepted that the reflection changes from regular to irregular as soon as sonic signals generated behind the reflection point catch up with the reflection point, and the common interpretation is that this corresponds to the transition from regular to Mach reflection (the so-called sonic criterion). The results obtained here for convex circular surfaces show that this 'catch-up' condition occurs at wall angles considerably higher than in the plane wall case, while a visible Mach stem occurs only further along the surface at wall angles distinctively lower than those for plane walls. Tests are also conducted on a surface where a cylindrical portion is followed by a fixed angle plane section. The Mach numbers are chosen to be on either side of the plane wall transition condition so as to examine the adjustment from reflection on the cylindrical portion to that on the plane wall. These tests confirm that the wall angle at which sonic 'catch-up' to the reflection point occurs on the cylindrical surface is much higher than the corresponding wall angle predicted by the sonic criterion for a plane wall. While the transition from regular to irregular reflection is not the main concern of this contribution, the present results show that the transition criteria developed for steady and pseudo-steady flows are only of limited use in the fully unsteady flows such as the one investigated here.

---

1. Introduction

When a plane shock wave impinges on a plane wall, the reflection patterns exhibited are well documented and for intermediate shock Mach numbers, as dealt with in this paper, are designated as regular reflection and single Mach reflection as shown in figure 1. Of pertinence to later discussion is the velocity of the flow behind the reflection point relative to the reflection point. In the case of regular reflection this velocity is supersonic and thus any small perturbation arising from the wall is swept

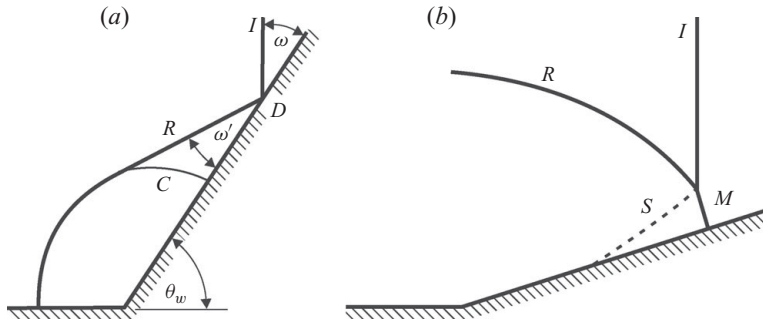† Email address for correspondence: beric.skews@wits.ac.za

FIGURE 1. (a) Regular reflection and (b) Mach reflection patterns. I is the incident shock, R is the reflected shock, M is the Mach stem, S is the slipstream, and C is the corner signal. θ_w is the wall angle, and ω and ω' are the incident and reflected shock angles in regular reflection, respectively.

away from the reflection point. The so-called corner signal is such a perturbation. It is the head of the compression wave that communicates the presence of the corner to the flow and moves at sonic velocity relative to the oncoming supersonic flow. In the case of Mach reflection, however, the flow behind the Mach stem is subsonic and thus any wall perturbation will immediately influence the shock. As the wall angle reduces, so does the flow velocity relative to the reflection point, and for a given shock Mach number, sonic velocity is reached at a certain wall angle. In this plane wall configuration, the corner signal reaches the reflection point, and the reflection pattern changes from regular to Mach reflection, if boundary-layer effects can be neglected. This is known as the sonic criterion, established by Hornung, Oertel & Sandeman (1979), and is generally accepted as the condition for the transition from regular to Mach reflection on a plane wall. Hornung *et al.* (1979) also introduced a length-scale condition that considers that if there is a characteristic length associated with the reflecting surface, this will link with the length of the Mach stem and the transition from regular to Mach reflection. Wall radius effects are evident in the current study but are only considered in relation to the flow becoming sonic relative to the reflection point and not to the transition conditions. It should be noted, however, that the experimentally determined sonic point as determined by Lock & Dewey (1989) does not coincide with the theoretical one, but is still found to be the condition for transition. Theoretical treatments are based on the oblique shock relations of von Neumann (1943) and are referred to as the two-shock and three-shock theories respectively for the two reflection patterns.

In the case of reflection off a curved wall, the monograph by Ben-Dor (2007) provides a comprehensive overview of all work published so far in this field. Experiments by Takayama & Sasaki (1983) on a variety of cylinders with different radii and initial wall angles are presented by Ben-Dor (2007), part of which are reproduced in figure 2. In all cases the experimental transition points are lower than what is predicted by the sonic criterion for a plane wall, which suggests that on a cylindrical surface the regular reflection pattern can be maintained down to smaller wall angles than for plane surfaces. An important point to note is that the transition point is obtained from images when an identifiable Mach reflection appears and therefore could depend on the scale of the experiment and the image resolution. If the visualization only provided single images, there is also an inherent uncertainty regarding the exact instant of the transition. For larger radii ($\geqslant 150$ mm) one observes
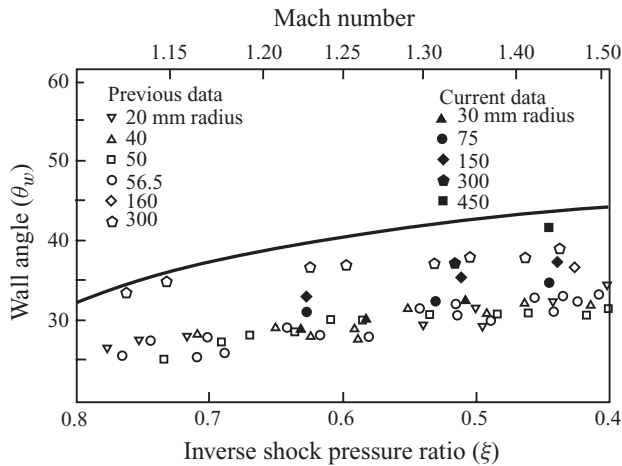
FIGURE 2. Wall angles at which Mach reflection becomes evident for different radii surfaces and shock strengths. The solid curve is the sonic criterion for plane walls. Previous data are from Ben-Dor (2007).

that the wall angle for transition increases with radius and that it approaches the sonic curve as should be expected. If it is assumed that the detection of a Mach stem is related to the optical resolution of the experiment, a Mach stem may be observed at higher wall angles if the flow pattern could be observed at much higher magnification as the stem gradually moves away from the wall. In this case the wall itself would appear less curved and the data of figure 2 would move towards the plane wall case. As normal-size shock tubes cannot accommodate complete cylinder models with large radii, one usually only investigates a partial model. The initial wall angle of these models does not influence the process as long as the initial reflection is regular and the reflection point outstrips the corner signal. In this case the corner signal stays behind the reflection point, which therefore has no knowledge of the existence of the starting angle. This is not in accordance with the data from Takayama & Sasaki (1983) in Ben-Dor (2007) as will be discussed later.

A few data points from the current tests are included in figure 2 and are consistent with the earlier data. However, it is not the point of this paper to examine the actual transition from regular to irregular reflection, that is, the experimental appearance of a Mach stem, but rather to examine reflected shock angles and to interrogate the conditions behind the reflection point, specifically during the regular reflection phase as a shock propagates up over the surface of the cylinder.

2. Experimental details

Experiments were conducted in a standard rectangular shock tube with a 150 mm high and 75 mm wide test section. The test gas is ambient air at nominal pressure and temperature of 95 kPa and 293 K. For time-resolved visualization, a schlieren/shadowgraph system was used in conjunction with a Shimadzu HPV-1 high-speed camera, which can record full-frame images at rates up to one million frames per second. Shock Mach numbers can be determined with an accuracy of ± 0.003. In order to determine the character of the flow, i.e. whether it is super- or subsonic with respect to the reflection point, small perturbation sources are placed transverse to the flow on the model surface (Skews & Kleine 2009). The sources
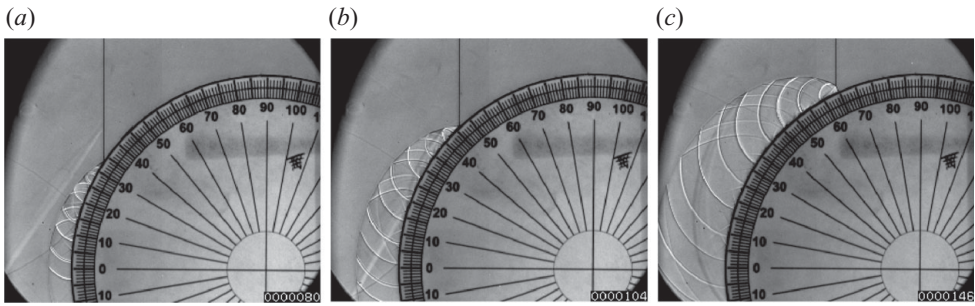
(a) (b) (c)

FIGURE 3. A Mach number 1.324 incident shock reflecting off a 75 mm radius cylinder showing the development of the perturbation signals. The full, time-resolved, schlieren visualization is supplementary movie 1. The number at the bottom right-hand corner of each frame is the elapsed time in microseconds. The front-lit model displays a graduated scale with the polar angle of the cylinder, which for regular reflection corresponds to the incidence angle ω.

consist of 45 μm thick transparent tape whose edges generate a weak wave in the following flow behind the shock. Part of this wave (termed the Q-wave) propagates down the surface against the oncoming flow induced behind the reflected wave and part, the P-wave, propagates up the wall but will only exist if the flow relative to the reflection point is supersonic. If this flow is subsonic the P-wave will immediately merge with the reflection pattern. The essential outcome from this technique is that it enables one to establish when the flow becomes sonic, that is, at which position the P-wave ceases to exist as an individual, discernible flow feature. This will be termed the 'catch-up' condition and should not be confused with the sonic criterion used for plane walls. The technique is illustrated in figure 3, and supplementary movie 1 (available at journals.cambridge.org/flm). This result is mainly shown for demonstration purposes, as the test model has been equipped with a large number of perturbation sources. Because of concerns regarding a possible influence on the flow by the presence of the perturbation sources, their number was usually kept to a minimum. The thickness of the tape is about 15 % smaller than the roughness size for which the surface can still be considered as hydraulically smooth (Ben-Dor *et al.* 1987). A second light source is used to illuminate a graduated scale attached to the side face of the model. The three still frames show the changing flow patterns. In the first frame there are six Q-waves propagating downwards and six P-waves upwards. In the second frame there are nine Q-waves since the shock has traversed a further three perturbation sources, but only seven P-waves. Thus, two of the new waves have merged with the reflected shock indicating that the flow behind the reflection point is now subsonic with respect to the reflection point. In the third frame there are eleven visible Q-waves plus two that have moved out of frame and the remaining seven P-waves. At this stage the transition to Mach reflection has occurred and a clear slipstream and Mach stem have become visible.

3. Results

Three different aspects are considered. First, using the perturbation technique, to establish the catch-up condition where a forward facing perturbation first merges with the reflected wave; second, to compare the reflected wave angles with those for a plane wall at the same wall angle (perturbations are not needed for these tests);
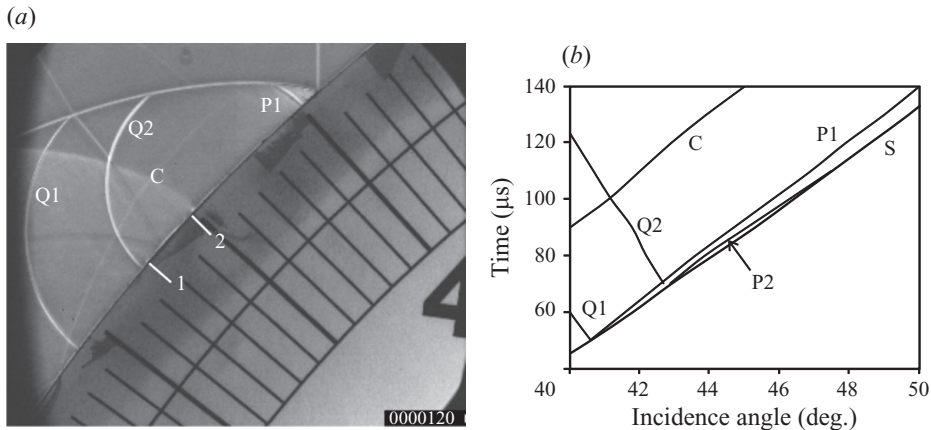
FIGURE 4. Schlieren image of the propagation of a shock along a 300 mm radius surface fitted with perturbation sources at positions 1 and 2, together with the corresponding wave diagram. The dynamic propagation of these wavelets throughout the reflection process can be seen in supplementary movie 2. Note that to obtain the angles on the wave diagram, 7.8° should be added to those on the photographic image because of a zero offset in mounting the model.

and third, to explore the transition if a curved wall segment is followed by a plane section of wall.

3.1. *Catch-up conditions*

Figure 4 shows a typical frame from a movie record and the associated method of analysis. In this case two perturbation sources are in place at positions marked 1 and 2. These are the edges of a single strip of tape. The backward-facing waves, Q1 and Q2, are clearly visible, as is the forward-facing P-wave from the lower perturbation source. At the time of this image the P-wave from source 2 has merged with the shock. Also noted on the photograph is the corner signal, C, arising from the entrance to the model which has been truncated with an initial wall angle of 32° in order to fit in the shock tube. This confirms that the initial angle is not a factor in the reflection process because the wave generated by the first engagement of the shock wave with the curved surface at this initial angle has not caught up with the reflection point.

From the time-resolved records, one can determine the position of the observed waves on the wall. These data can then be plotted in a modified x–t diagram (wave position at the cylinder wall as a function of time), where the main modification lies in choosing the incidence angle instead of the actual spatial coordinate. In transferring the data from the movie to the wave diagram 7.8° was added to the angle because of a zero-scale offset in mounting the model. Such a wave diagram is constructed tracking the position of the perturbations, the shock and the corner signal as shown in figure 4. The P2 wave initially diverges from the shock trajectory which indicates that the flow behind the reflection point is initially supersonic when the shock passes over perturbation source 2. However, its velocity then equals and eventually exceeds that of the shock so that the P2 wave catches up with the reflection point. From an assessment of where a perturbation starts to where it catches up to the shock, an estimate may be made of the position where the flow behind the shock becomes sonic. Such diagrams enable better estimates to be made of the catch-up values. It is estimated that this result will be accurate to within $\pm 1°$.
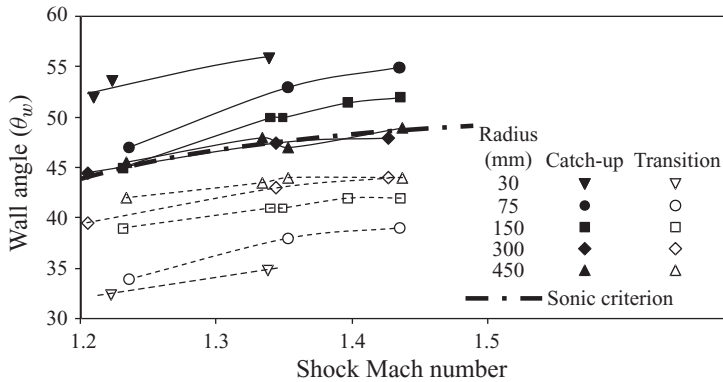
FIGURE 5. The catch-up and visible transition conditions for a range of wall radii.

The results for these tests are given in figure 5. This shows both the catch-up angle and the transition angle at which a Mach stem becomes visible for the cases tested, as well as the sonic criterion for a plane wall. For large wall radii, the experimentally determined sonic catch-up angles correspond to the theoretical value for a plane wall, but are still significantly different from where a Mach stem appears. For small radii, the catch-up occurs much earlier along the surface, and the difference to the angles at which a visible Mach stem appears is even greater, amounting to as much as 20° for the smallest radius of 30 mm. Both angles, catch-up and transition to Mach reflection, increase as the Mach number increases, and therefore follow the trend predicted by the sonic criterion. This result suggests that a more complex flow process is occurring behind the reflected wave than previously assumed.

A further means of highlighting this difference and the influence of the cylinder radius is by the measurement of reflected wave angles. Such measurements do not require the use of perturbations.

3.2. *Reflected shock angles*

For small radii, there is a marked difference between the sonic catch-up values determined above, the plane wall sonic criterion, and the visible appearance of a Mach stem, and hence there will also be a difference in the flow immediately behind the reflected wave. This will have an effect on the reflected wave angle which thus also needs to be compared. Although the image resolution of the high-speed camera is rather low and angle measurement subject to some error, consistent data are obtained as shown in figure 6. It is recognized that angle measurement on curved waves can often be an estimation rather than a precise measurement, as has been shown in high-resolution calculations (Timofeev *et al.* 1999) but this is standard practice in experiments, such as those of Smith (1945), when comparisons of reflection patterns are made.

At small incidence angles, it is only the smallest radii that show a difference from the theoretical regular reflection case, but at higher angles the deviation increases significantly as the radius decreases. It should be noted that even for the plane wall case, experimental results begin to deviate from the theoretical curve at high incidence angles (Smith 1945) in much the same way, due to boundary layer growth as identified by Hornung *et al.* (1979). The range of test results shown for the test pieces with large radii is smaller than that for the smaller models, because the test section could only accommodate partial models. Consequently, the incident shock entered at a higher
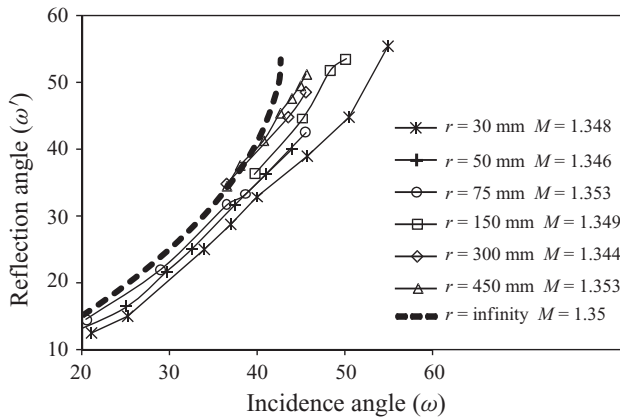
FIGURE 6. Reflection angles for regular reflection off cylinders of various radii at a nominal shock Mach number of 1.35.
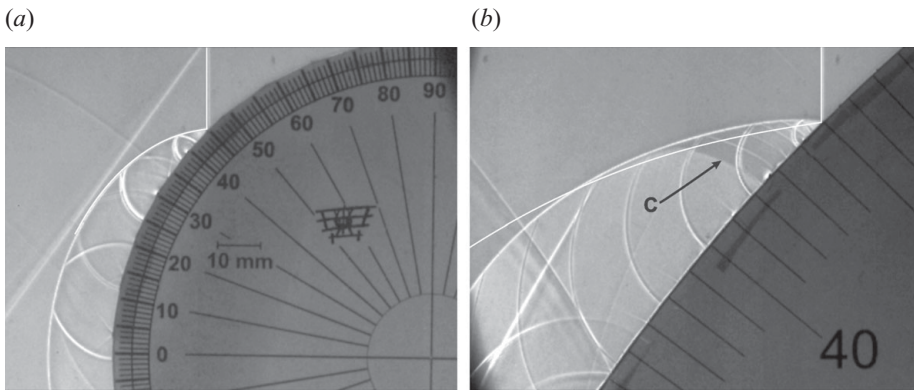
(*a*)   (*b*)

FIGURE 7. (*a*) Comparison of reflected shock profiles for a Mach 1.353 incident shock at 45° incidence on a 75 mm and a 450 mm radius cylinder. (*b*) The reflected wave from the first image is magnified 600 % and superimposed on the second. C is the corner signal.

starting incidence angle, but this does not affect the results as long as the reflection point outstrips the corner signal. The effect of radius influence on the whole of the shape of the reflected wave is shown in figure 7. Two of the results at Mach 1.353 with the incident shock at an incident angle of 45° are compared between tests on radii of 75 mm and 450 mm. The reflected shock profile is traced from the 75 mm case, expanded by the ratio of radii (600 %) and superimposed on the 450 mm case. It is not only the angle of reflection that is influenced by the radius as shown in figure 6 but, as shown, the whole reflected shock profile. The flows are clearly not self-similar and Reynolds number effects are thus evident. The comparison of the reflected shock profiles should only be made up to the point where for the larger model the corner signal (C in figure 7) begins to influence the shock. This corner signal only exists for the large model, but does not appear for the smaller one.

3.3. *Transition from curved to straight walls*

The theoretical sonic criterion predicts that at a 45° wall angle, transition to Mach reflection will occur at a Mach number of 1.2318. However, in practice there is a persistence of regular reflection and this transition occurs at a slightly larger

(*a*)   (*b*)   (*c*)
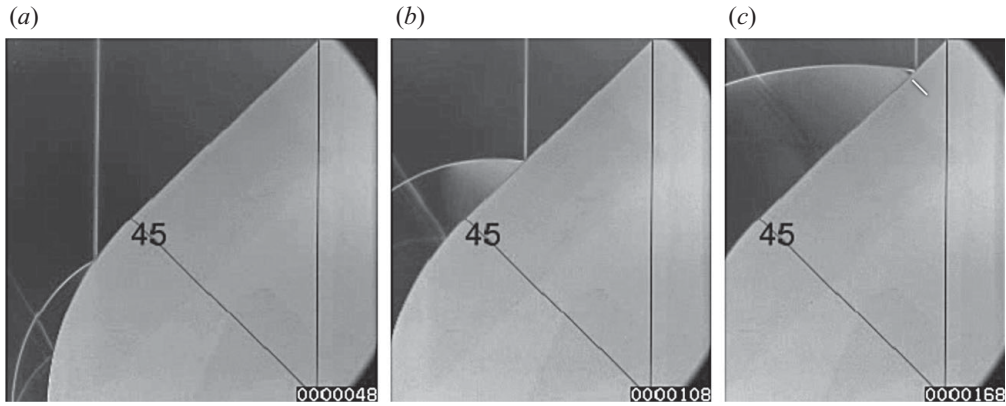

FIGURE 8. Propagation of a Mach 1.230 incident wave over a compound wall consisting of a circular cylinder with 75 mm radius followed by a plane wall at 45° inclination. The position of a new corner signal is identified by the short white line in the third image. The number at the bottom right-hand corner of each frame is the elapsed time in microseconds. The temporal evolution can be seen in supplementary movie 3.

incidence angle (Smith 1945), due to boundary layer growth behind the reflection point (Hornung *et al.* 1979). A detailed discussion of the effect of boundary layers on plane walls is given in Ben-Dor (2007). This has the consequence of changing the actual sonic point, as shown by Lock & Dewey (1989), who used a single perturbation technique similar to that in this work, the main difference being that their perturbations were generated independently of shock transit. Thus, the Mach number for transition on a 45° wall is likely to be between 1.25 and 1.3. For the circular wall with 75 mm radius, the previously described tests indicate that catch-up has already occurred above a wall angle of 45° for this entire Mach number range, while the visible appearance of a Mach stem is consistently below this angle. Thus, the combination of a leading 75 mm radius wall followed by a 45° plane surface will give further insight into the transition conditions. Two such tests have been conducted at Mach numbers of 1.23 and 1.336. In both cases, according to the tests described in § 3.1, the sonic catch-up will already have occurred on the circular portion. On the basis of the results shown earlier, one would expect that on the following straight surface, the pattern remains that of a regular reflection for the lower Mach number while it should change to Mach reflection in the higher-Mach-number case. Conversely, if the catch-up were equivalent to transition from regular to Mach reflection, a Mach reflection pattern should also become evident in the low-Mach-number case.

Figure 8 shows three frames from the movie for the Mach 1.23 test, which is available online. (The white line visible at the left side of the frames is a transverse wave caused by the diaphragm rupture. As it trails the incident shock by a distance of several tens of millimetres, it has no influence on the flow at the wall. The propagation and nature of this wave, very common in shock tube testing, also become obvious from the movie clip.) The three frames are separated by 60 μs. As shown before, catch-up has occurred in the first frame and there is no sign of any transition in the second. However, at an instant between the ones shown in the middle and right frames in figure 8, when the incident shock has propagated about halfway up the plane surface, a new corner signal emerges, which subsequently clearly separates from the reflection point. Its position at a later time is indicated in the right frame of figure 8. This signal arises from the discontinuity in curvature where the circular arc
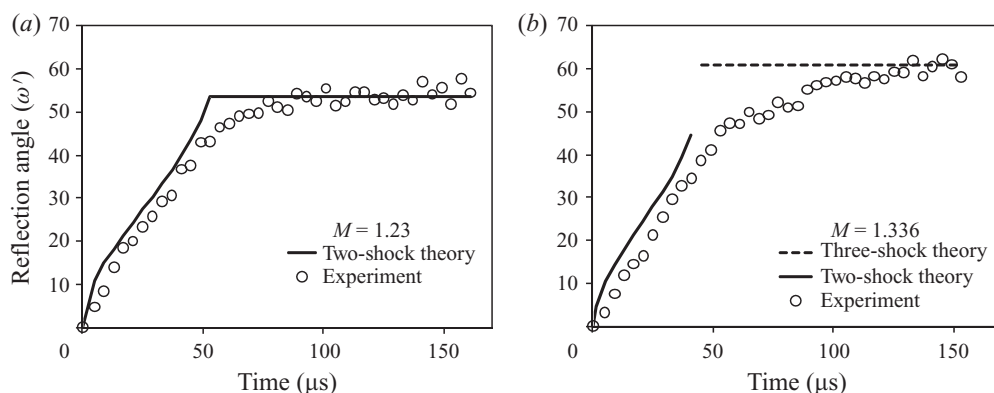
FIGURE 9. Comparison between the experimental and theoretical reflected wave angles for two Mach numbers, one on either side of the Mach number for plane wall transition conditions, thus one tending to regular reflection and the other to Mach reflection.

merges with the plane wall. Thus, the flow has once more become supersonic relative to the reflection point, thereby leaving any wall perturbations behind. This is positive confirmation of the early catch-up of perturbations on the circular arc. For the case of the Mach 1.336 test, there is no direct evidence of the appearance of a Mach reflection but the reflected shock angle is continually increasing as shown below. This indicates that the pattern approaches that of a Mach reflection, which is expected to become visible only at larger distances, i.e. for a larger test model. Confirmation of this is given in figure 9, where the reflected angles for the two tests are compared with theoretical predictions.

For the Mach 1.23 case, the two-shock theory applies slightly beyond a wall angle of 45° and so the sudden kink in the theoretical curve corresponds to where the variation in wall angle along the circular section changes to a fixed wall angle with an associated predicted constant reflection angle. From the measured wall angles, it becomes obvious how the shock pattern gradually transitions from reflecting from a curved surface to a straight one. The slightly lower reflection angles on the curved portion are consistent with previous findings. Using the data of Smith (1945) for $M = 1.254$ ($\xi = 0.6$) as a guide, it would be expected that the experimental data would asymptote to a value slightly higher than the theoretical curve, because of the persistence of regular reflection, but the scatter in the current tests resulting from the low image resolution does not allow a conclusion in this regard.

For the Mach 1.336 case, a wall angle of 45° is above both the sonic and detachment conditions and thus the two-shock theory prediction terminates whilst the incident shock is still on the curved part of the surface. The three-shock theory for this wall angle is shown and the reflected shock angle is measured with respect to the triple point trajectory, which for this case is 1.24° above the surface. The experimental results show a smooth transition towards the three-shock case. Again, using the Mach 1.363 ($\xi = 0.5$) case of Smith (1945) as a guide, it could be expected that the experimental data would asymptote to a value slightly below the theoretical prediction, and that a Mach stem would appear in the experiment if the model were longer.

Further evidence of this gradual transition from the catch-up condition on the circular arc to the eventual well-known conditions on a plane wall can be obtained from an analysis of the flow deflection and Mach number variation behind the reflected shock using the experimentally measured shock angles. The results are shown in figure 10.
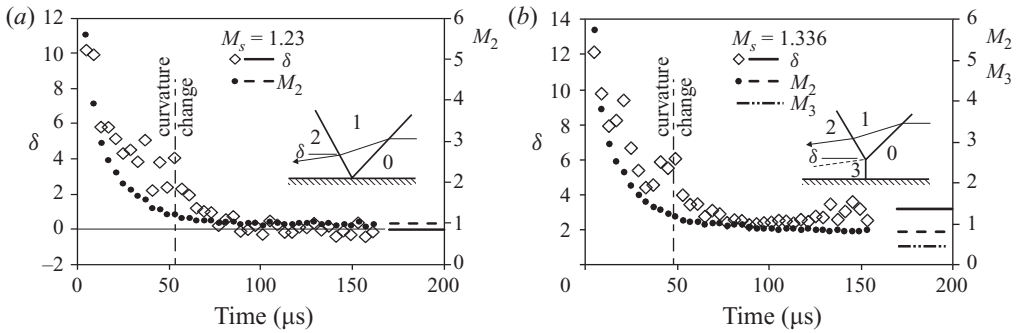
FIGURE 10. Flow deflection and Mach number variation behind the reflected shock derived from the experimental reflected shock angles. The straight lines on the right of the plot are the theoretical values for a plane wall at an angle of 45°.

Calculations are done using the two-shock theory of von Neumann (1943). As the theory assumes a plane reflected wave, which is clearly not the case here, the results should only be seen as an indication for flow direction and Mach number. There is scatter in the deflection angle data arising from the measurement uncertainty of shock reflection angle but clear trends emerge. There is a significant flow direction towards the wall in the early part of the interaction where wall angles are steep, and this reduces as the point of curvature changes from the circular arc to the plane wall but is still inwards there. It then reduces further as the flow adjusts to the presence of the plane wall.

For the Mach 1.23 case, where the reflection is regular on a plane wall, the data asymptote to the theoretical values both in terms of zero flow deflection and the theoretical Mach number behind the reflection point of 1.005 (Fig. 10a). This result, along with the appearance of the new corner signal shown in figure 8, confirms that the flow has adjusted from the flow around the curved section to that on the plane wall. The result for the stronger incident shock is compared with the theoretical predictions from the three-shock theory (Fig. 10b), which is fairly accurate at this Mach number. It is notable that the deflection angle, after what appears to be a slight drop, tends towards the theoretical angle of the shear layer of a Mach reflection at this wall angle and incident shock Mach number, $\delta = 3.17°$, and the Mach number behind the reflected shock clearly tends towards the theoretical value of 0.822. Thus, although a Mach reflection has not yet become visible in the experiments, all the boundary conditions for it to exist are satisfied, and it may simply be that it is too small to be resolved and that it would become visible in an experiment with a longer straight section of the model.

4. Conclusion

The main conclusion of this work is that an area of flow behind a shock reflecting off a convex circular surface of small radius becomes subsonic relative to the reflection point much earlier than would be expected from considerations of the sonic criterion on plane walls or from inferences resulting from the appearance of a Mach stem. There is clearly a complex flow evolution between where this catch-up occurs and where a visible transition between regular and Mach reflection becomes evident. For the case of a plane wall, the persistence of regular reflection has been ascribed to the influence of the boundary layer developing behind the shock (Hornung *et al.* 1979). Because of the no-slip condition at the wall and the fact that the reflection point is moving supersonically along the wall, this means that in a frame of reference fixed

in the reflection point the flow at the wall is supersonic whereas it is slower further out. The result is a negative displacement thickness allowing an apparent inflow towards the wall and an increase in the reflected shock angle. If the flow outside of the boundary layer is sonic, or slower, then downstream information will catch up with the reflection point. This condition is generally accepted as the condition for transition from regular to Mach reflection for the plane wall case. For the curved wall case considered here, the situation is more complex, for up to the catch-up condition found, i.e. before the change of slope in figure 10, the flow at the wall is supersonic because of the boundary-layer effect, but so is the flow immediately behind the reflected wave. However, as the reflected wave is convexly curved, the flow processed by it is converging and therefore slowing down. As the incident shock progresses up the wall, the flow behind the reflected shock will therefore, at some point, become subsonic. Thus, it is envisaged that a subsonic patch will develop which will grow in time and allow some downstream disturbances to catch up. The nature, growth and extent of this region need to be investigated. Higher resolution time-resolved physical experiments than those currently available will allow higher accuracy results to be obtained than those presented here but are unlikely to shed significant further information on the immediate post-shock flow. Computational simulation becomes necessary, requiring very high-resolution numerical experiments in order to resolve the eruption of a Mach stem, the development of the boundary layer and the evolution of the sonic line. However, even then it is difficult to ascertain accurately when a Mach stem erupts or where the flow becomes sonic behind the reflection point because of the finite size of the cell elements in a computational grid. Some promising approaches to address this issue in the case on an inviscid calculation have been given by Timofeev *et al.* (1999) and Hakkaki-Fard & Timofeev (2009). A programme of numerical investigations to explore such issues has been initiated.

Supplementary movies are available at journals.cambridge.org/flm.

REFERENCES

BEN-DOR, G. 2007 *Shock Wave Reflection Phenomena*. Springer.

BEN-DOR, G., MAZOR, G., TAKAYAMA, K. & IGRA, O. 1987 Influence of surface roughness on the transition from regular to Mach reflection in pseudo-steady flows. *J. Fluid Mech.* **176**, 336–356.

HAKKAKI-FARD, A. & TIMOFEEV, E. 2009 High resolution determination of sonic and detachment angles at shock wave reflection from a circular cylinder. In *Proceedings of 17th Annual Conference of the CFD Society of Canada*. Paper CFDSC2009-4D3.

HORNUNG, H. G., OERTEL, H. & SANDEMAN, R. J. 1979 Transition to Mach reflexion of shock waves in steady and pseudosteady flow with and without relaxation. *J. Fluid Mech.* **90**, 541–560.

LOCK, G. D. & DEWEY, J. M. 1989 An experimental investigation of the sonic criterion for transition from regular to Mach reflection of weak shock waves. *Exp. Fluids* **7**, 289–292.

VON NEUMANN, J. 1943 Oblique reflection of shocks. *Tech. Rep.* 12. Bur. Ord. Explosives Research.

SKEWS, B. W. & KLEINE, H. 2009 Unsteady flow diagnostics using weak perturbations. *Exp. Fluids* **46**, 65–76.

SMITH, L. G. 1945 Photographic investigation of the reflection of plane shocks in air. *Tech. Rep.* 6271. Office of Scientific Research and Development.

TAKAYAMA, K. & SASAKI, M. 1983 Effects of radius of curvature and initial angle on the shock transition over concave and convex walls. *Tech. Rep.* 46. Institute of High Speed Mechanics, Tohoku University, Sendai, Japan.

TIMOFEEV, E., SKEWS, B. W., VOINOVICH, P. A. & TAKAYAMA, K. 1999 The influence of unsteadiness and three-dimensionality on the regular-to-Mach reflection transitions: a high-resolution study. In *Proceedings of the 22nd International Symposium on Shock Waves* (ed. G. J. Ball, R. Hillier & G. T. Roberts), pp. 1231–1236. University of Southampton, UK.